American Journal of Engineering Research (AJER)
e-ISSN: 2320-0847 p-ISSN: 2320-0936
Volume-15, Issue-2, pp-35-43
www.ajer.org
Research Paper Open Access

Amorphous ternary alloys Si Ge B in thin film deposited by LFPECVD morphology and electrical properties

Ernesto Franco Pastrana, and Alfonso Torres Jacome
Ele3ctronics Deoartment, National Institute for Astrophysics Optics and Electronics, INAOE, Tonatzintla, Pue., Mexico, C.P. 72480

Abstract. *a-SiGeB alloys are deposited by means of LPCVD at low frequency (100 kHz) at a deposition temperature of 200 °C. After annealing at 500 °C in a forming gas environment, the electrical conductivity increases up to three orders of magnitude with respect to as-deposited films. This is explained by the incorporation of dopants to the amorphous lattice, as demonstrated by FTIR studies. Through Raman spectra, it is determined that the alloy is composed mainly of Ge and boron, with a few incorporations of silicon. From the results here obtained, the amorphous phase is maintained even after 500 °C annealing; therefore, the high electrical conductivity obtained and the low thermal conductivity expected because the alloy resulted in amorphous films make this material a good candidate as a thermoelectric material for thermoelectric generators in addition to the already known applications.*
Keywords: *a-SiGeB:H alloys, electrical conductivity, stoichiometry, Raman spectra.*

Date of Submission: 01-02-2026 Date of acceptance: 10-02-2026

I. Introduction

Amorphous silicon germanium alloys (a-SiGe:H) are a kind of material that has been used in very different and interesting applications such as optoelectronic detectors, thin film transistors, solar cells, microbolometers, and thermoelectric materials. Their deposition as a thin film by using PECVD at low temperatures (less than 400 °C) makes this material compatible with the current technologies of integrated circuit fabrication. The introduction of a highly conductive silicon germanium boron (Si-Ge-B) ternary amorphous alloy in 1982 by K. Murase [1], deposited by glow discharge decomposition, in which the ratio GeH4/SiH4 of gases entering the deposition system was in the range of 0.2%—2%, resulted in a high conductivity alloy and also showed increasing values of the Seebeck coefficient as the Ge content increases. It is also important to mention that Murase et al. just doped the a-SiGe alloy with a gas phase ratio of B_2H_6/SiH4 from 2×10^{-3} to to 5×10^{-2}, which is only doping the alloy.

In this work we use a much higher Ge content and up to 9% B incorporation in order to form a SiGeB alloy for reducing the resistivity of it. At the same time, the microcrystallization is avoided. That is, maintaining the amorphous quality of the material. In this case the alloy is deposited in an LPCVD system at low frequency (110 kHz) at 200 °C of deposition temperature. The electrical and structural characteristics are studied as a function of the B content.

II. Materials and Methods

All the samples were deposited by PECVD capacitivedischarge system (AMP-3300 of Applied Materials) at RF frequency of 110 kHz, its power density was$90\mathrm{mW/cm^2}$ (RF power = 300 W) with a deposition temperature T_s = 200 °C. The percentage in gas phase (B_{gas}) of Diborane(B_2H_6at 1% diluted in H_2) was determined by the Eq. (1) and the dilution rate (R) was defined by Eq. (2), where Q is the gas flux in sccm, additionally the percentage of GeH_4 in gas phase (X_g) wascalculated with Eq. (3)

$$B_{gas} = Q_{B_2H_6} \times 100/(Q_{SiH_4} + Q_{GeH_4}) \quad (1)$$

$$R = Q_{H_2}/(Q_{SiH_4} + Q_{GeH_4}) \quad (2)$$

$$X_g = Q_{GeH_4} \times 100/(Q_{SiH_4} + Q_{GeH_4}) \quad (3)$$

The conditions for deposition of the film with the lowest dilution Ratio (R = 4) were: deposition times t_d= 60 min, chamber pressure P_d= 0.6 Torr, $B_{gas} = 4$ and$X_g = 0.6$. For the remainder of the films, the depositing conditions were: P_d= 1.2 Torr, t_d= 60 min, $X_g = 0.9$ the dopant percentages, B_{gas}, were in a range from 4% to 9% (show in Table 1). The total flow of Silane(SiH_4) and Germane(GeH_4) were 125 sccm and 50 sccm for the lowest dilution ration and the rest of the films. After LPCVD deposition the films were subjected to an annealing at a temperature (T_a) of 500°C, inside an electric oven with a quartz chamber in forming gas atmosphere (N_2 60% and H_2 40%) for 60 minutes. The room-temperature conductivity (σ_{RT}) was measured using source meter model 2401 of Keithley with 4-wire sensing and the thickness was estimated by using a profilometer model Dektak XT of Bruker. The a-SiGe:H films were deposited on substrates of Silicon wafer with 200 nm of grown oxide, and Corning glass 2947.

The IR absorption spectra of the films were measured with an infrared spectrometer Thermo scientific, model Nicolet iS50 FT-IR in the range 400–4000 cm^{-1}, on the other hand Raman spectra were obtained by Raman microscope WiTec alpha 300 R. Si wafers without oxide and with 200 nm of grown oxide were used as substrates for FTIR and Raman characterization respectively.

The micrographics was done by scanning electron microscope (SEM) through microscope FEI, model Scios, the chemical composition measurement was obtained by secondary ion mass spectrometry (SIMS), the measurements were carried out by using a spectrometer TOFSIMS-5.

III. Results and discussion

Conductivity

The typical value of conductivity for hydrogenated amorphous germanium is $1\times 10^{-4}cm^{-1}\Omega^{-1}$ but the for the amorphous ternary SiGeB alloy the value reported value is $1 \times 10^{2}cm^{-1}\Omega^{-1}$[1].

In the table I the electrical conductivity of the here-deposited films is presented before and after the annealing of the films. There is a three orders of magnitude larger conductivity for the annealed films over the same films without annealing. The reason for this is that after deposition, not all the dopant atoms are in a site in the amorphous lattice; therefore, these remain un-ionized and do not contribute carriers to the conduction. The hydrogen is necessary to reduce the dangling bonds because it acts as a deep trap (D^0). When thetemperature of the annealing is higher than 200°C, the effusion of hydrogen starts; hence, the passivated dopants$(H-B_4^0) + (T_4^0 - H)$which were not incorporated to the lattice, lose hydrogen and get a dangling bond. If two dangling bonds have enough distance to make a bond (1.4 Å) [2] and the coordination number reach a value near of 4, the activation of dopant occur ($B_4^- - T_3^+$).

According to a computational study [3] the tetrahedral configuration (hybridized sp_3) is the most stable configuration for B atoms is the tetrahedral configuration. Therefore most of the boron atoms produced a carrier (hole). The reaction also depend of the distance, for this reason, more thermal energy (for the diffusion) is necessary to activate the dopants and increase conductivity, the change of electrical conductivity [4].

TABLE1DEPOSITION PARAMETERS OF BORON DOPED SAMPLES AND ELECTRICAL CONDUCTIVITY (σ_{RT}),.

B_{gas}	R	Deposition fluxes		σ_{RT}	σ_{RT} T_{an}= 500° C
		H_2	B_2H_6		
(%)	(dimen - sionless)	(sccm)	(sccm)	($cm^{-1}\Omega^{-1}$)	($cm^{-1}\Omega^{-1}$)
4	4		500	0.0657	2.894[1]
4	20	800		3.25×10^{-3}	1.404[1]
6	20	700	300	5.11×10^{-3}	1.63
7	20	650	350	5.73×10^{-3}	1.17
8	20	600	400	5.39×10^{-3}	1.81
9	20	550	450	4.51×10^{-3}	3.23
8	15	350	400		4.67×10^{-2}
8	10	100	400		2.72×10^{-2}

Raman Spectra

The Raman spectra were smoothed using OriginPro 2018 software, andspectral deconvolution was applied to obtain five characteristic peaks associated with amorphous Germanium. Since the film predominantly consists of Ge, the identified vibrational modes correspond to longitudinal optical (LO), longitudinal acoustic (LA),

transverse optical (TO), and transverse acoustic (TA) phonons. These peaks do not correspond to the phonon modes at the Brillouin zone center typically observed in crystalline germanium (c-Ge), as the lack of long-range order in amorphous solids removes translational symmetry.

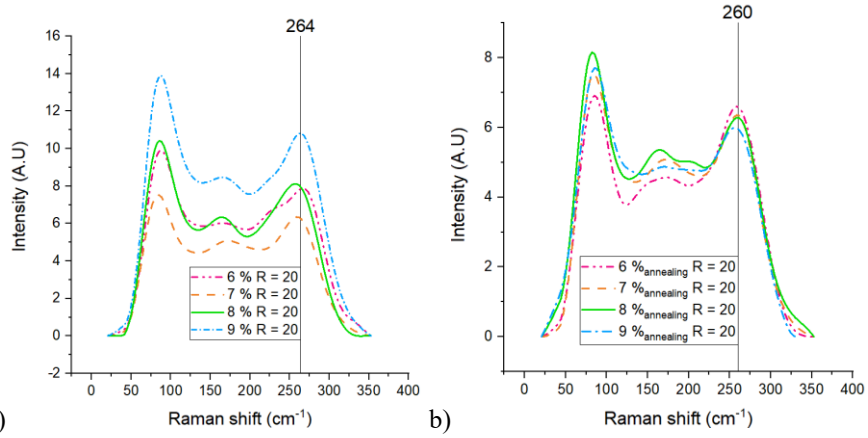

a) b)

Figure 1. Raman spectra of amorphous Ge, Si and B alloys for various values of B in gas phase B_{gas} from 0 to 400 cm^{-1} of a) before annealing, b) after annealing.

However, the vibrational density of states in amorphous Ge still reflects features analogous to those in the crystalline phase [5]. A fifth peak, observed at 110 cm^{-1} and referred to here as x, in the literature is attributed to the vibrational mode of the Ge_3–GeH bonds, which is normally located near 120 cm^{-1}.

The vibrational and electrical properties are domain for the molecular structure, for this reason the Raman spectra of amorphousSi and Ge are related with the vibrational states of their crystalline phase, this occurs because domains the effects of short-range order (SRO). For the amorphous phase the Raman and infrared spectra can simulateonly withSRO effects and theabsence of longer range effects [5].

A study of density functional perturbation theory(DFPT) in a crystalline lattice with two nanostructures pores and nanowire of Ge shows that the surface vibrational states contribute to a large extent to the vibrationalproperties near the highest optical modes, even though the number of hydrogen bonds in the surface of nanostructures changes [6].The Raman spectra of the amorphous ternary SiGeB alloys deposited at low frequency PECVD are shown in the Fig. 1 and Fig. 2, the characteristic peak at 280 cm^{-1} of a-Ge does not appear in the Raman spectra, this change is related to the boron incorporation but, also there are not peaks in the amorphous binary SiGe alloy deposited at the same conditions (see Fig. 2).

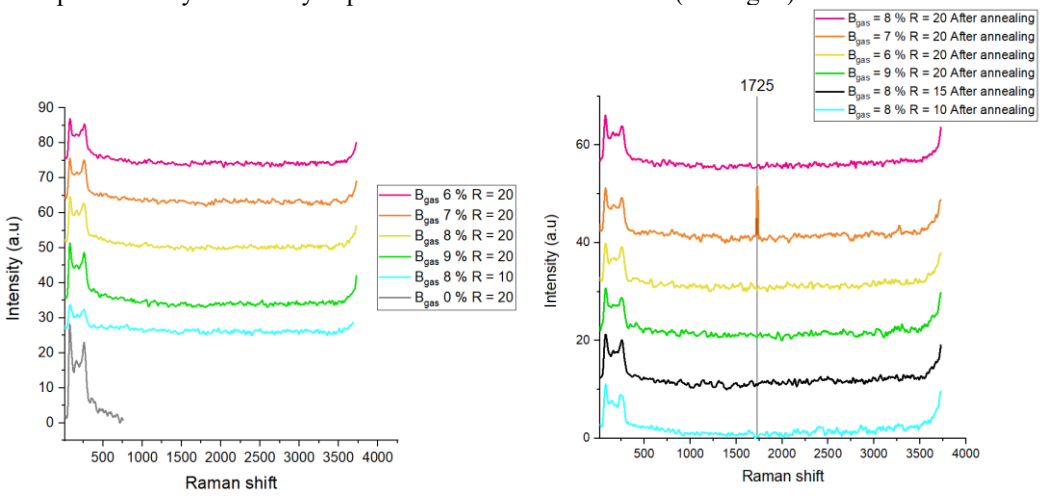

a) b)

Figure 2. Raman spectra of amorphous Ge, Si and B alloys for various values of B in gas phase B_{gas} from 0 to 4000 cm^{-1} of a) before annealing, b) after annealing.

The characteristic modes of carbon lie between 1100 and 1800 cm^{-1} [7] as can be seen from figure 2 only the annealed film doped at 7% has a peak at 1725 cm^{-1}, therefore this sample may be contaminated with C, in the FTIR(see Figure 4),the peak at 1550 cm^{-1}is associated with C-B bonds. On the other hand, in the FTIR

spectra, peaks between 2800 and 3000 cm^{-1} were not observed, this range is attributed to C-H_1, C-H_2 and C-H_3 stretching modes [7], hence the C concentration may be low, or the peaks could be related with other phenomenon.

Boron, at high concentrations, tends to form icosahedrons, such as the rhombohedral β boron, its Raman spectra have a characteristic peak at 1223 cm^{-1} [8]. Furthermore, the peak at 1100 cm^{-1}, is ascribed to amorphous boron (a-B), more specifically is also attributed to internal vibrations of the icosahedral. However, these peaks are not observed in the Raman spectrum shown in figure 2, only the peaks of a-Ge:H appear. Therefore, the lattice of the films should be a similar molecular structure of hydrogenated amorphous Germanium (a-Ge:H), consequently their coordination number may be near of the value of a-Ge:H(3.8 to 4.1).

The vibrational states of the material are intimately connected with the Raman spectra, if the peak is not present, then the more energetic states (TO modes) of the material are localized, as a result, the peak moves to less energetic states (move to left). As a result the characteristics TO mode peak of a-Ge moves from 280 $cm^{-1}$to 265 cm^{-1}.

The metastable tetragonal Ge III (st-12) appears in Raman spectra of a samples after a plastic deformation using high-pressure torsion (HPT) under a pressure of 24 GPa, the Ge III phase enhanced by the shear strain [9]. The Raman spectra shows a characteristic st-12 Ge peaks in nanowire of Ge [10]

In the table II and III the St-12 Ge peak values are compared with the value of the modes, which was obtained deconvolution of Raman spectra of the Fig.1, the position that vary more than 10 cm^{-1} are marked in grey

TABLE II DECONVOLUTION PEAKS OF RAMAN SPECTRA

	Raman deconvolution			
St-12 Ge [5]	**B_{gas} = 6%**	**B_{gas} = 7%**	**B_{gas} = 8%**	**B_{gas} = 9%**
(cm^{-1})	(cm^{-1})	(cm^{-1})	(cm^{-1})	(cm^{-1})
55				
85, 90	TA = 82.54	TA = 80.9	TA = 78.34	TA = 80.43
100	x = 110.6	x = 112.67	x = 99.71	x = 101.81
	LA = 172.87	LA = 166.23	LA = 160.87	LA = 166.6
190				
210		LO = 208.72		LO = 219.3
230	LO = 222.95		LO = 229.6	
257	TO = 267.54	TO = 269.52	TO = 268.23	TO = 265.99
275				

TABLE III RAMAN SPECTRA DECONVOLUTION PEAKS OF ANNEALED FILMS

	Raman deconvolution			
St-12 Ge [5]	**B_{gas} = 6% T_{an}= 500° C**	**B_{gas} = 7% T_{an}= 500° C**	**B_{gas} = 8%T_n= 500° C**	**B_{gas} = 9%T_{an}= 500° C**
(cm^{-1})	(cm^{-1})	(cm^{-1})	(cm^{-1})	(cm^{-1})
55	TA = 68.72			
85, 90	x = 86.44	TA = 79.06	TA = 78.84	TA = 82.2
100		x = 106.9	x = 102.3	x = 114.66
	LA = 151.97	LA = 169.18	LA = 167.17	
190				LA = 188.11
210		LO = 210.27	LO = 206.23	
230	LO = 219.6			LO = 226.21
257	TO = 265.53	TO = 259.79	TO = 258.43	TO = 264.91
275				

We can see that most of the peaks have a similar value of the St- 12 Ge, the reason may be related with grow of the film, the formation of nanopowder occurwhen the pressure is above to 0.9 Torr. These nanostructures disrupt the nucleation of the film and the powder are embedded in the amorphous film. This may be related to the aspect of the surface in the SEM micrographs in the Fig. 3.

The diameters of the nanoclusters were measured using ImageJ software by analyzing the grayscale intensity profiles along the yellow line. The diameters presented in Table IV show no correlation with the doping level, as indicated by a Pearson correlation coefficient of 0.1472, which is close to zero.However, these

structures are expected to alter the surface vibrational states, resulting in a shift of the TO peak toward lower wavenumbers.

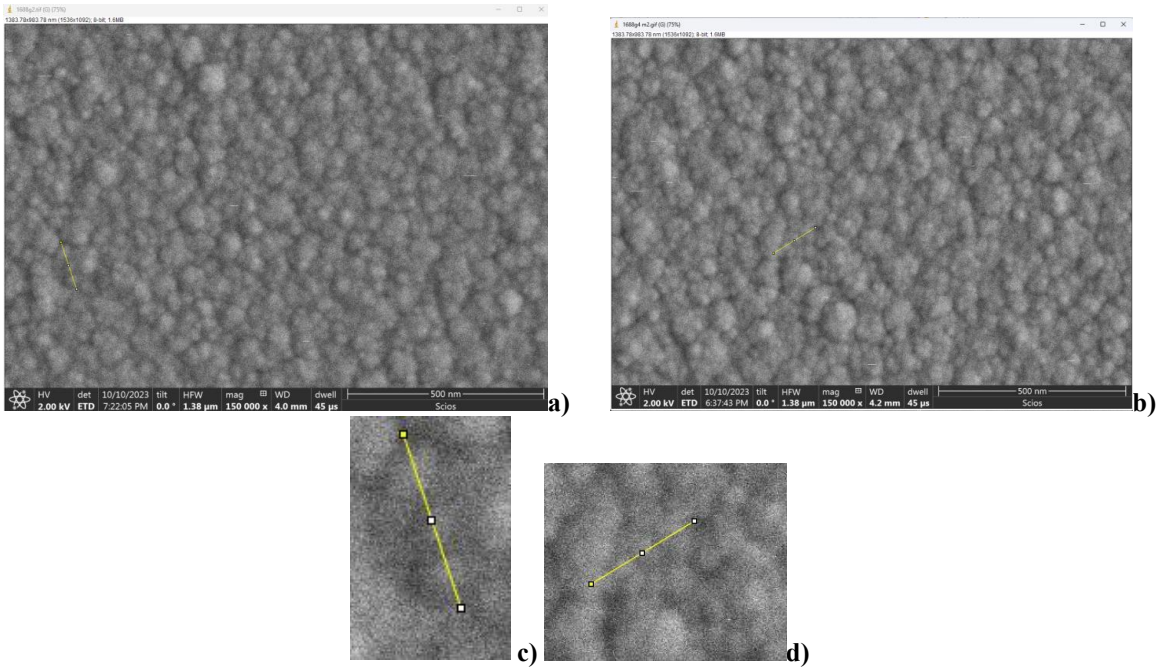

Figure. 3 SEM micrographs a) B_{gas} = 7 %, b) B_{gas} = 9 %, c) zoom around yellow line of B_{gas} = 7 % and d) zoom around yellow of B_{gas} = 9 %.

TABLE IV NANOCLUSTER DIAMETERS

Samples	Cluster diameter (nm)
B_{gas} = 6%	25.57
B_{gas} = 7%	38.74
B_{gas} = 8%	26.79
B_{gas} = 9 %	31.83

FTIR

The FTIR spectra shown in Figures 4 to 6 were smoothed and baseline corrected using OriginPro 2018 software. The peaks between 560 and 1880 cm^{-1} are attributed to bending and stretching modes of Ge-H bonds respectively [11], whereas the peak at 1100 cm^{-1} is ascribed to Si-O. After annealing the peak at 560 cm^{-1} is reduced, while the peaks, attributed to GeH, GeH_2 and GeH_3 [12], are localized in 1880, 1970, and 2050 cm^{-1} disappear [12, 13]. This fact makes evident the effusion of hydrogen from the film. The peak near 2500 cm^{-1} is attributed to B-H stretching modes that do not form hydrogen bonds between boron atoms [14] other peak that appears in , its presence indicate that the material has a high boron concentration and after annealing the peak disappear, which indicate that the hydrogen passivated dopants are activated by hydrogen effusion, through formation of dangling bonds. As a consequence two dangling bonds interact to produce weak bonds, which become alternation valence pairs $(T_3^0)+(B_4^0\text{-}H)\rightarrow(T_3^+\text{-}B_4^-)$, this weak bond breaks and become in two open bonds, one positively charged and the other negatively, these charged bonds act as shallow traps that reduce the activation energy, therefore with a little energy it is possible to release the trapped carriers, as a result their concentration increase and also the electrical conductivity. The formation of alternation valence pairs will only occur if the dopants have a coordination number of 4; otherwise, if they have a coordination number of 3, they become deep traps that reduce electrical conductivity.

The 820 cm^{-1} and 1290 cm^{-1} peaks give us a first approximation of what proportion of the boron atoms have a coordination number of 4. The 820 cm^{-1} peak is attributed to BO_4, while the peaks at 1290 cm^{-1} are attributed to BO_3 [15]. It can be observed that the peak at 820 cm^{-1} is larger than the peak at 1290 cm^{-1}. The conclusion is that there are more BO_4 molecules than BO_3. After deposition, the films are exposed to the environment, where oxygen is introduced into the film.

After annealing, the film is released into the room environment at 200°C, again oxygen is introduced into the film. Unlike the growth of silicon oxide, with germanium oxide, oxygen is incorporated through an exchange of oxygen atoms, oxygen goes out of the GeO_2 film (desorption), and oxygen from the environment is incorporated into the film. This process is controlled by oxygen vacancies that diffuse to the film surface. Typically, deposition conditions primarily influence the film structure, with substoichiometric oxygen desorption of the film, hence oxygen most likely only diffuses through the film without modifying the

coordination number of the a-Ge:H matrix, i.e., both Ge and B atoms already have an established coordination number (3 or 4) and oxygen only enters the open bonds. So, more boron atoms may have a coordination number 4 (B_4) instead of 3 (B_3), because B_3 atoms have a higher energetic cost [16]. As a consequence, electrical conductivity increases after hydrogen effusion, since there are more B atoms with a coordination number of 4.

The annealing also changes the position of some peaks, some examples are: peak from 657 to 680 cm^{-1}, peak from 820 to 830 cm^{-1} and other peaks practically disappear as example: the peak in 1678 cm^{-1}, peak at1700 cm^{-1}, peak at 1655 cm^{-1} except for the sample with B_{gas} = 7 %, the peak at 1763 change and increase in 1768 cm^{-1}, for the rest of the sample disappear.

The peak in 1700 cm^{-1} is larger in the three samples with $B_{gas} = 8\%$, this peak was reported in other ternary, in the article shows a relation with the peaks near of 1850 cm^{-1}, for films with: $B_{gas} = 4\%$, R=4, in a X_g value range from 0.33 to 0.6, Pd = 0.06 Torr at 300°C. In our samples, this relation is not present. On the other hand, an interesting relation with electrical conductivity lies in the peak at 1655 cm^{-1}. If the peak is large the conductivity will be high, but after annealing the peak disappears. Except in the film with B_{gas} = 7 %, which have the largest value of resistivity after annealing.

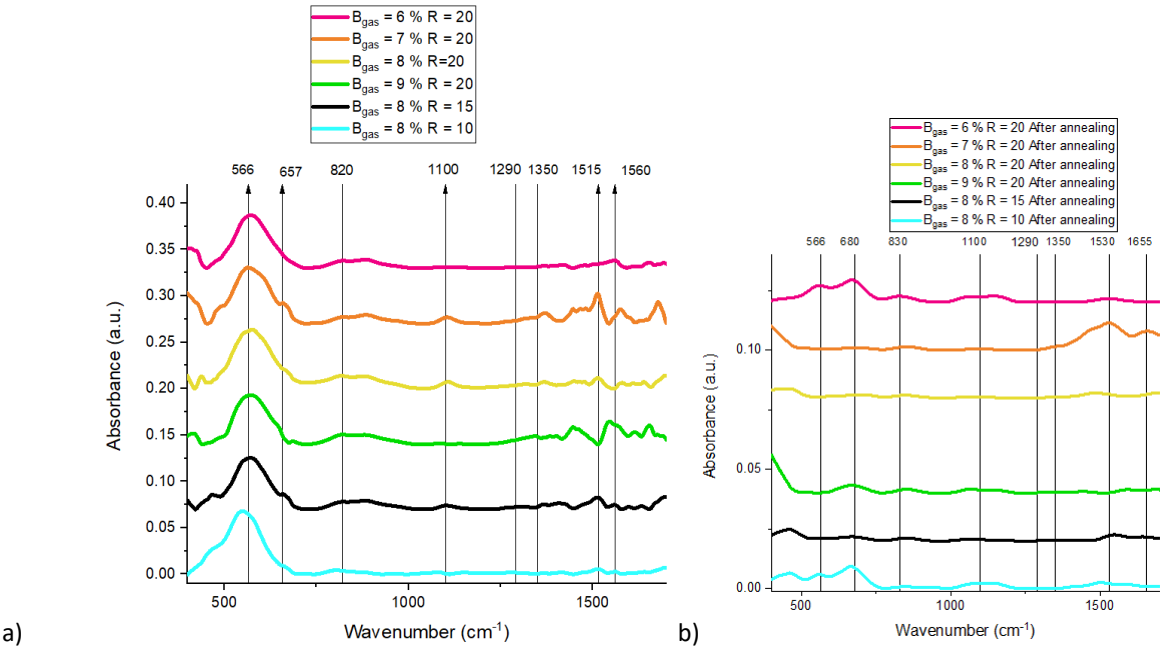

Figure 4. FTIR absortion spectra of amorphous Ge, Si and B alloys for various values of B in gas phase B_{gas} from 400 to 1700 cm^{-1} of a) before annealing, b) after annealing.

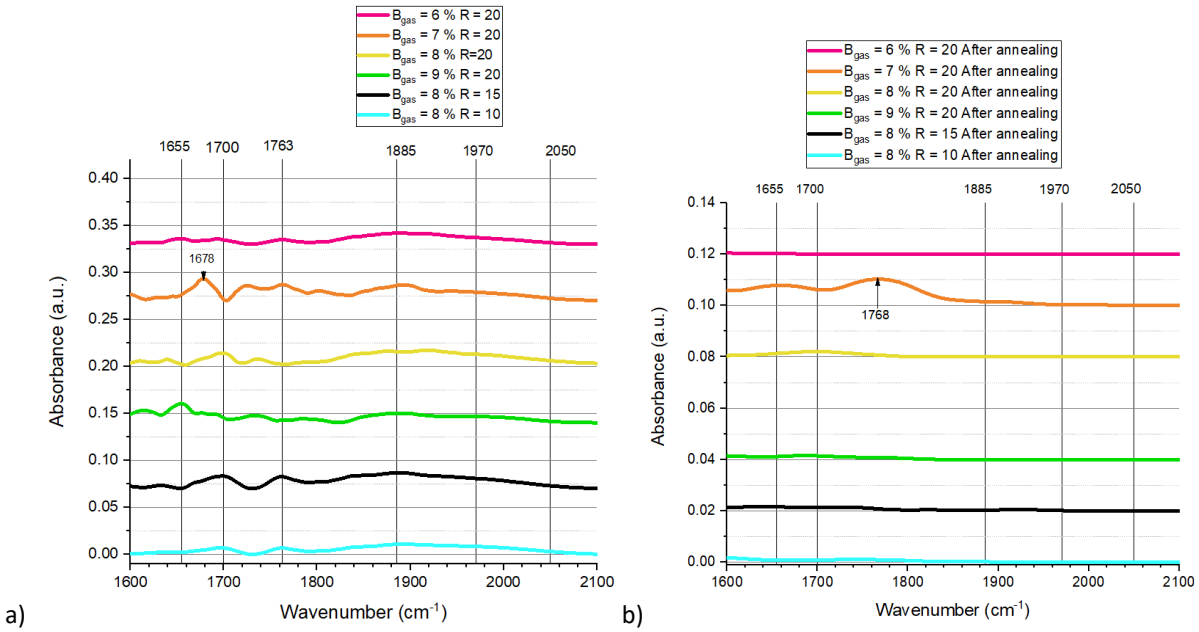

Figure 5. FTIR absortion spectra of amorphous Ge, Si and B alloys for various values of B in gas phase B_{gas} from 1600 to 2100 cm^{-1} of a) before annealing, b) after annealing.

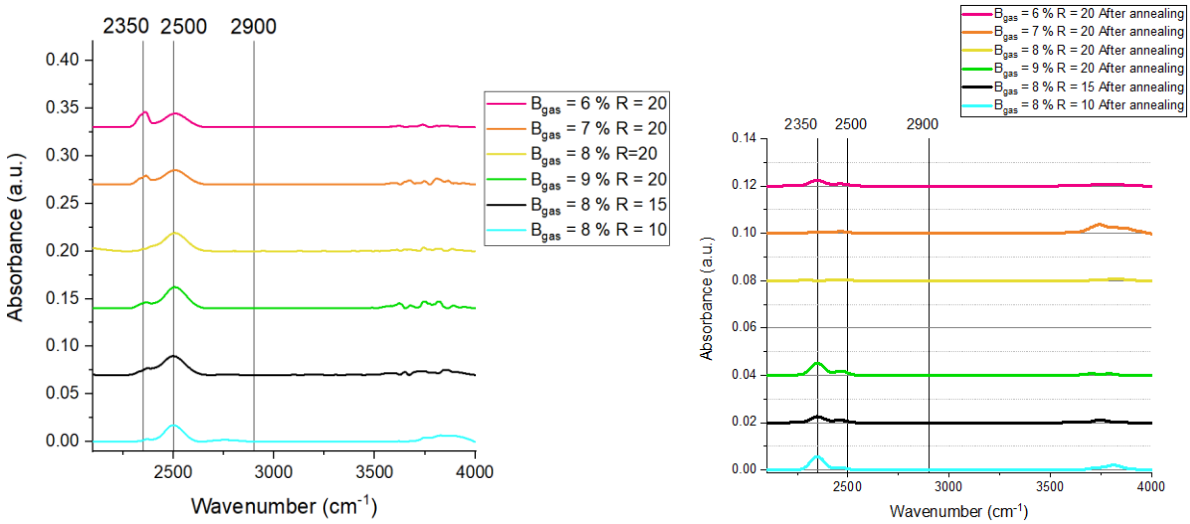

Figure 6. FTIR absortion spectra of amorphous Ge, Si and B alloys for various values of B in gas phase B_{gas} from 2100 to 4000 cm^{-1} of a) before annealing, b) after annealing.

IV. Conclusions

The room temperature electrical conductivity of LPCVD-deposited a-SiGeB alloys increases up to three orders of magnitude after annealing at 500 °C in a forming gas environment with respect to as-deposited films. This is explained by the incorporation of dopants to the amorphous lattice, as demonstrated by FTIR studies. Through Raman spectra, it is determined that the alloy is composed mainly of Ge and boron, with a few contributions of silicon. From the results here obtained, the amorphous phase is maintained even after 500 °C annealing, therefore the high electrical conductivity obtained and the low thermal conductivity expected because the alloy resulted in amorphous films make this material a good candidate as a thermoelectric material for thermoelectric generators.

Acknowledgment

The authors would like to acknowledge the financial support provided by CONACHYT through scholarship No. 794442. We also extend our sincere gratitude to the personnel of the Microelectronics and Microscopy Laboratories at INAOE, with special thanks for their valuable assistance to: Victor Aca Aca, José Juan Aviles

Bravo, Armando Flores Hernández, Ignacio JuárezRamírez, Leticia TecuapetlaQuechol and Carlos Ramirez Netzahualcoyotl.

References

[1]. Murase, K., Takeda, A., &Mizushima, Y. (1982). Silicon-germanium-boron ternary amorphous alloy. *Japanese Journal of Applied Physics*, *21*(4R), 561.

[2]. J. Boyce, S. Ready, and C. Tsai, "Local structure of dopants in compensated and singly-doped amorphous silicon," *Journal of Non-Crystalline Solids*, vol. 97, pp. 345–348, 1987.

[3]. P. Fedders and D. Drabold, "Theory of boron doping in a-si: H," *Physical Review B*, vol. 56, no. 4, p. 1864, 1997.

[4]. Franco, E., Torres, A., & Moreno, M. (2023, July). Increasing the doping efficiency by post-deposition annealing in a-SiGe: H films synthesized by PECVD. In *2023 IEEE Latin American Electron Devices Conference (LAEDC)* (pp. 1-4). IEEE.

[5]. Alben, R., Weaire, D., Smith Jr, J. E., & Brodsky, M. H. (1975). Vibrational properties of amorphous Si and Ge. *Physical Review B*, *11*(6), 2271.

[6]. Trejo, A., & Cruz-Irisson, M. (2013). Computational modeling of the size effects on the optical vibrational modes of H-terminated Ge nanostructures. *Molecules*, *18*(4), 4776-4785.

[7]. Jamali, H., Mozafarinia, R., &Eshaghi, A. (2015). Evaluation of chemical and structural properties of germanium-carbon coatings deposited by plasma enhanced chemical vapor deposition. *Journal of Alloys and Compounds*, *646*, 360-367.

[8]. Werheit, H., Filipov, V., Kuhlmann, U., Schwarz, U., Armbrüster, M., Leithe-Jasper, A., ...&Korsukova, M. M. (2010). Raman effect in icosahedral boron-rich solids. *Science and Technology of Advanced Materials*, *11*(2), 023001.

[9]. Ikoma, Y., Toyota, T., Ejiri, Y., Saito, K., Guo, Q., &Horita, Z. (2016). Allotropic phase transformation and photoluminescence of germanium nanograins processed by high-pressure torsion. *Journal of Materials Science*, *51*, 138-143.

[10]. Raha, S., Srivastava, D., Biswas, S., Garcia-Gil, A., Karttunen, A. J., Holmes, J. D., &Singha, A. (2021). Probing lattice dynamics in ST 12 phase germanium nanowires by Raman spectroscopy. *Applied Physics Letters*, *119*(23).

[11]. Yu-Pin Chou and Si-Chen Lee. Structural, optical, and electrical properties of hydrogenated amorphous silicon germanium alloys. *Journal of applied physics*, *83*(8):4111–4123, 1998.

[12]. Arrais, A., Benzi, P., Bottizzo, E., &Demaria, C. (2009). Correlations among hydrogen bonding configuration, structural order and optical coefficients in hydrogenated amorphous germanium obtained by x-ray-activated chemical vapour deposition. *Journal of Physics D: Applied Physics*, *42*(10), 105406.

[13]. Serényi, M., Frigeri, C., Csik, A., Khánh, N. Q., Németh, A., &Zolnai, Z. (2017). On the mechanisms of hydrogen-induced blistering in RF-sputtered amorphous Ge. *CrystEngComm*, *19*(11), 1486-1494.

[14]. Tsai, C. C. (1979). Characterization of amorphous semiconducting silicon-boron alloys prepared by plasma decomposition. *Physical Review B*, *19*(4), 2041.

[15]. Marzouk, S. Y., Seoudi, R., Said, D. A., &Mabrouk, M. S. (2013). Linear and non-linear optics and FTIR characteristics of borosilicate glasses doped with gadolinium ions. *Optical Materials*, *35*(12), 2077-2084.

[16]. Fedders, P. A., &Drabold, D. A. (1997). Theory of boron doping in a-Si: H. Physical Review B, 56(4), 1864.